

## ASH FALL PREDICTION IN NEW ZEALAND

T. Poirot<sup>1</sup>, J. Cole<sup>1</sup> & D.G. Elms<sup>2</sup>

### ABSTRACT

The North Island of New Zealand contains seven active volcanoes or volcanic centres, and ash fall from these centres could present health hazards and other problems. Part of the required contingency planning for ash fall is the assessment of the frequency and depth of ash fall at any point. The issue is particularly important for urban areas likely to be affected. This paper develops a theory for ash fall frequency assessment based on estimated eruption frequencies and magnitudes and on meteorological data. The theory is used to obtain the ash fall frequency/depth relationship for the Napier/Hastings area in the Hawkes Bay region. The results show that the annual frequency of significant ash fall in the towns is high enough to justify some degree of emergency preparedness, with a fall of 1 mm having an annual exceedance probability of about 0.05, or in other words a return period of approximately 20 years.

**Keywords:** ash fall hazard, probability, frequency, prediction

### INTRODUCTION

Ash fall is a natural hazard that could affect large areas in the North Island of New Zealand, where there are a number of active or dormant volcanoes and volcanic centres. Following an eruption, ash fall could affect human health, property and community infrastructure. It is therefore essential in the planning of civil defence and emergency management strategies and prioritisations that the hazard should be understood and assessed as well as possible, both qualitatively as to what could happen and quantitatively as to the level and degree of risk.

Hitherto, analysis of ash fall hazards has generally been carried out in a deterministic manner utilising scenario approaches. While this could give significant and useful information as to the nature of the effects of ash fall should it occur, such information is inadequate from the point of view of prudent planning because it gives no indication of the relative seriousness of different risks. Yet prudent planning and management of the community's finite resources cannot be carried out systematically without first being able to assess and prioritise the risks, which in turn requires quantification.

This paper gives a methodology for assessing the probability of ash fall occurrence of a given thickness at a certain point arising from a number of volcanic sources. Specifically the probability of ash fall occurrence of 1, 5, and 50 mm is assessed at Napier/Hastings in the Hawke's Bay region arising from the Tongariro Volcanic Centre (TgVC), Egmont

Volcanic Centre (EVC), Taupo Volcanic Centre (TVC) and Okataina Volcanic Centre (OVC) (Figure 1). Past ash fall deposits preserved in lakes and bogs in the region are predominantly derived from these centres. The methodology developed represents an alternative approach to previously developed models concerning ash fall hazards in the North Island of New Zealand (for example, Latter, 1985; Johnston & Nairn, 1993; Johnston, 1997; Dalziel, 1998; Scott *et al.*, 1998; Rhoades *et al.*, 2002). Although the Napier/Hastings area is used here, the model can also be used to determine the probability of ash fall occurrence of a given thickness at any point in the North Island potentially subject to ash falls from these volcanic centres.

The main aim of the research was not so much to produce a finished product as to develop and prove a methodological approach, which could be refined at a later stage, and could be widely used throughout New Zealand. The results are useful for Hawkes Bay, but both the data and the degree of detail could and should be further refined. The main finding of the work is that the method is workable.

### MODEL OVERVIEW

The model of the annual probability (i.e. frequency) of ash fall occurrence of a given thickness at a certain point combines two main components. The first is a set of annual occurrence probabilities of eruptions of different sizes occurring at the different volcanic centres in the North Island, while the second component contains probabilities of

<sup>1</sup> Dept. of Geological Sciences, University of Canterbury, Christchurch, New Zealand

<sup>2</sup> Dept. of Civil Engineering, University of Canterbury, Christchurch, New Zealand (Member)

occurrence of different wind directions and wind speeds at different heights. Wind direction and wind speed give the direction and distance the ash will travel. Different scenarios were constructed for different combinations of parameters.

Ash fall thickness was then calculated deterministically for different points for each scenario using the computer program ASHFALL, described below.

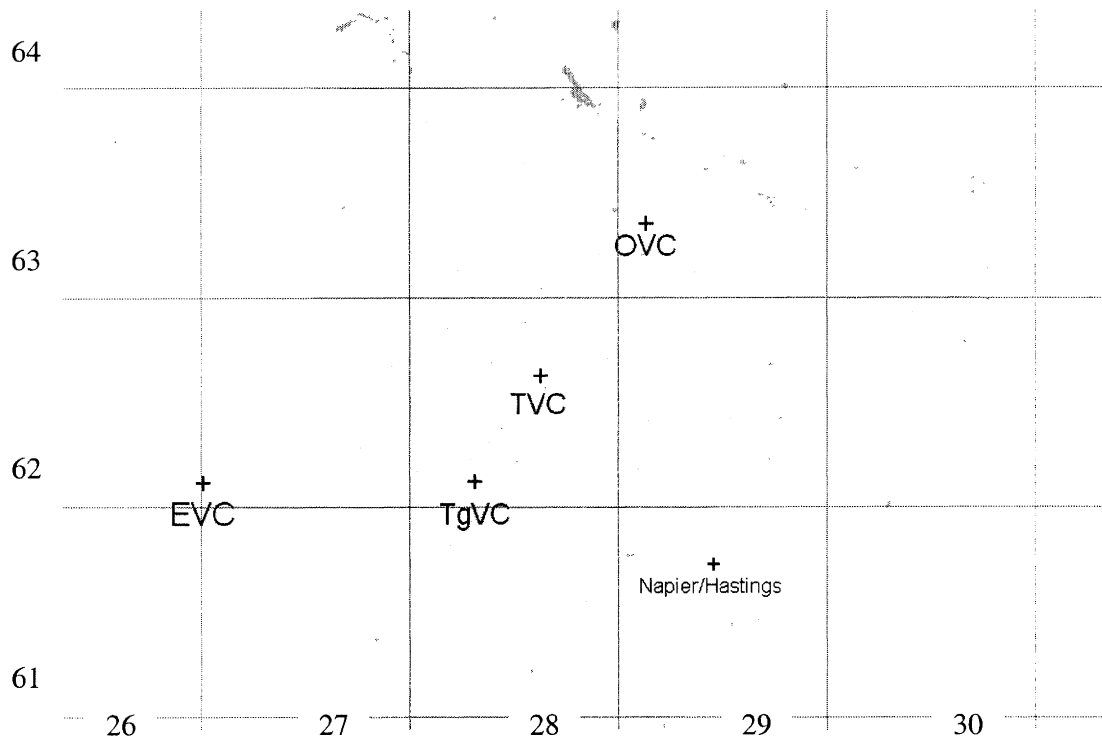


Figure 1. Volcanic centre locations.

Each scenario has a different frequency of occurrence, depending on eruption and wind statistics. The scenarios and their frequencies can then be combined to find the annual exceedance probability of a given ash fall thickness at any required location, and specifically, in this study, for the Napier/Hastings region.

A number of simplifying assumptions were used in the model, and these are discussed below. The aim was to balance the degree of uncertainty in the data with the degree of approximation of the model, following the methodological principle of consistent crudeness (Elms, 1992). This principle states in essence that the uncertainty ("crudeness") of a result is primarily determined by the model input or data with the greatest degree of crudeness, and not by an averaging process. Thus there is no point in constructing a model that is more refined than the level determined by the least reliable data – further refinement of the model would not improve the accuracy of the results, even though it might give a spurious indication of precision. This principle is the basis of most of the simplifying assumptions in the theory presented below.

#### ASHFALL – COMPUTATION OF ASH FALL THICKNESS

The computer program used in this study was ASHFALL, a DOS-based program developed by the Institute of Geological and Nuclear Sciences (IGNS) to predict the thickness of ash fall at any one point, resulting from different eruption sizes occurring from different volcanic centres, under different wind conditions (Hurst, 1994). The program is based on work done by Armienti *et al.* (1988) and Macedonio *et al.* (1988) with regard to the distribution of volcanic ash. It does not consider the effects of other volcanic hazards such as lava flows, pyroclastic flows and surges, debris avalanches and lahars. During the 1995-1996 eruptions of Mt. Ruapehu, ASHFALL was used to predict the thickness of ash fall, based on forecasted wind conditions provided by the Meteorological Service of New Zealand, Ltd. (Hurst & Turner, 1999). Careful analysis of three well-defined eruption events showed that the thickness of ash fall at any one point was generally within a factor of two (attributed to errors in the forecasting of wind conditions) of the predicted results, so validating the program's potential usefulness (Hurst & Turner, 1999).

## LOCATION

ASHFALL starts by assuming an explosive eruption, which produces an eruption column containing a certain erupted volume of ash, measured in cubic kilometres. The eruption column rises as an isolated thermal plume to the height ( $H_B$ ) at which its density equals that of the surrounding atmosphere. Above this height, the eruption column continues to ascend to a maximum height ( $H_T$ ) due to its excess momentum, but will slump back towards its level of neutral buoyancy ( $H_B$ ), at which the ash spreads out horizontally in the atmosphere and settles under gravity.

The distribution of ash with height in ASHFALL is assumed to follow the Suzuki distribution (Hurst, 1994), which indicates that the maximum concentration of ash will occur near the top of the column, that is, between heights  $H_B$  and  $H_T$  (Hurst & Turner, 1999). The thickness of ash fall at any one point is obtained by taking into account how the concentration of ash is influenced by different wind conditions as it begins to settle under gravity.

In order to obtain the thickness of ash fall at any one point, ASHFALL divides all ash particles into classes with similar settling velocities. The horizontal position of each class will change as it begins to settle under gravity and is influenced by different wind conditions. Once particles within a class reach the ground, the distribution of the class is calculated based on its horizontal movement through the air. Each class will have a different horizontal movement because of different settling velocities. The quantities of ash from all the classes are combined at points on a two-dimensional rectangular grid, giving an area-wide distribution of ash fall thickness.

Use of ASHFALL requires the input of three main items of information, namely:

1. The location of the eruption column,
2. The total erupted volume and maximum column height, and
3. The wind direction and wind speed at each level between the ground level and the maximum height of the eruption column.

It was assumed that eruptions could take place at the four locations identified in the Introduction. The positions of the eruption columns were defined using the New Zealand Map System (NZMS) grid coordinates as follows:

TgVC	27313E	62105N
EVC	26018E	62116N
TVC	27654E	62656N
OVC	28144E	63346N

The locations of these points are shown in Figure 1. Note that the major grid lines shown on the figure are spaced at 100 km intervals, and that the Napier/Hastings area is located at 28447E 61763N.

### Erupted volumes and column heights

It has been observed that the maximum column height is positively correlated with the total erupted volume (Carey & Sigurdsson, 1989). Total erupted volumes of 0.01, 0.1 and 1.0 km<sup>3</sup> were used in this study. The Volcanic Explosivity Index (VEI) (Newhall & Self, 1982) was used as a general indicator to match total erupted volume with maximum column height. According to the VEI, total erupted volumes of 0.01, 0.1 and 1.0 km<sup>3</sup> would imply column heights ranging from 1-5, 3-15 and 10-25 km, respectively (Table 1). The overlapping ranges between column heights of successive VEI categories reflect the interaction between various eruption parameters, such as magnitude and intensity (Newhall & Self, 1982). However, when considering total erupted volumes of 0.01, 0.1 and 1.0 km<sup>3</sup> to be used in this study, a single maximum column height from each VEI category was used. Total erupted volumes of 0.01, 0.1 and 1.0 km<sup>3</sup> therefore correspond to maximum column heights of 5, 15 and 20 km respectively. A maximum column height of 20 km was used instead of 25 km, because both the National Institute of Water and Atmospheric Research (NIWA) and the Meteorological Service of New Zealand Ltd. only collect wind direction and wind speed data up to 20 km, limiting the eruption size that could be modelled. In reality, if an explosive eruption in the range VEI 5-6 (column height greater than 25 km) were to occur, as has happened prehistorically in the North Island, the hazards, including ash fall, would be widespread and highly damaging. It is not within the scope of the model to consider such large magnitude eruptions.

Table 1. Eruption sizes, column heights and return periods for the TgVC, EVC, TVC, and OVC (modified from Newhall & Self, 1982; Scott *et al.*, 1998).

Volcanic Centre	Size (km <sup>3</sup> )	Volcanic Explosivity Index (VEI)	Column Height (km) (VEI)	Return Period (years)
TgVC	0.01	2	1-5	20
	0.1	3	3-15	100
	1.0	4	10-25	10000
EVC	0.01	2	1-5	300
	0.1	3	3-15	1500
	1.0	4	10-25	10000
TVC	0.1-1.0	4	10-25	1500
	1.0-10	5	>25	2500-5000
	10-100	6	>25	5000-10000
OVC	0.1-1.0	4	10-25	1500
	1.0-10	5	>25	1500-2000
	10-100	6	>25	2000-5000

### Wind

The third set of data required for ASHFALL is the wind direction and velocity at different levels from the ground to the maximum height of the eruption column. Wind direction and wind speed indicate the direction and distance the ash

will travel. Upper atmosphere wind conditions are often different from lower atmosphere wind conditions and it is important to get a complete wind profile between the ground level and the maximum height of the eruption column. Three data sets of wind conditions were obtained from NIWA:

- |    |              |                 |    |                  |
|----|--------------|-----------------|----|------------------|
| 1. | Gisborne     | 1 February 1988 | to | 7 January 2001   |
| 2. | New Plymouth | 1 July 1984     | to | 7 January 2001   |
| 3. | Auckland     | 1 January 1966  | to | 31 December 1988 |

Each of these data sets consisted of one reading of wind direction (measured in degrees from true north) and wind speed (m/s) per day at altitudes of 5, 10, 15 and 20 km, taken using a combination of radar and wind-sounding balloons. The three data sets were combined and used in ASHFALL.

The combined data set was also used to determine the probability of occurrence of different wind directions and wind speeds over the North Island (see below). It is assumed that the combined data set will be representative of the typical distribution of wind directions and wind speeds over the North Island and is sufficient to characterise the general nature of them, as required for the model. Although ASHFALL also has the capability to include changes in wind conditions over the duration of an eruption, the wind

conditions are assumed to remain constant in our calculations.

### Wind Direction

Wind directions at heights of 5, 10, 15 and 20 km were also divided into eight 45° sectors. The probability of occurrence of wind within each of the eight sectors at each height is shown in Table 2. Probabilities greater than 0.20 are shown in bold case.

**Table 2. Wind direction probabilities at 5, 10, 15 and 20 km.**

Wind Direction	5 km	10 km	15 km	20 km
0-45°	0.04	0.02	0.01	0.07
45-90°	0.02	0.01	0	<b>0.20</b>
90-135°	0.03	0.02	0	0.16
135-180°	0.07	0.04	0.01	0.07
180-225°	0.16	0.13	0.07	0.06
225-270°	<b>0.28</b>	<b>0.35</b>	<b>0.46</b>	<b>0.20</b>
270-315°	<b>0.27</b>	<b>0.34</b>	<b>0.40</b>	0.16
315-360°	0.13	0.09	0.05	0.08

Table 2 shows that the wind direction probabilities at 5, 10 and 15 km are greatest in the two sectors 225-270° and 270-315°; that is, the wind is predominantly northwest to southwest. At 20 km the situation is different. It can be seen that the probability of occurrence is greatest in the 45-90° and 225-270° sectors.

This is not unexpected because the atmosphere can be divided into a number of well-defined horizontal layers, mainly on the basis of temperature. The lower layer of the atmosphere is the troposphere, where temperature falls with increasing height. The second layer is the stratosphere, in most of which the temperature remains constant with height. The stratosphere extends upwards from the troposphere to

about 50 km (Barry & Chorley, 1992; Sturman & Tapper, 1996). The interface between the troposphere and the stratosphere is termed the tropopause, which occurs at about 10 km at temperate latitudes. The tropopause is a temperature inversion layer, keeping the troposphere contained and effectively limiting convection between the troposphere and stratosphere. At 20 km, winds will be in the stratosphere where wind directions can be significantly different to those in the troposphere due to different atmospheric motions (Barry & Chorley, 1992; Sturman & Tapper, 1996).

#### Wind speed profiles

Carey & Sparks (1986) showed that wind speed will have a significant effect on the geometry of ash thickness contours, so four wind speed profiles were constructed from the combined data sets of wind conditions (Figure 2), with each profile indicating a probability band. The profiles were constructed by first plotting the distribution of wind speeds at 5, 10, 15 and 20 km, and then by plotting the wind speeds in each of the four quartiles up to the 99.5% confidence interval (0-25%, 25-50%, 50-75% and 75.0-99.5%) for each of the above distributions. The mean of each quartile at each of the respective heights was taken, and the wind speeds between these heights at levels of 1000 m were interpolated to produce the profiles of wind speed vs. height shown in Figure 2.

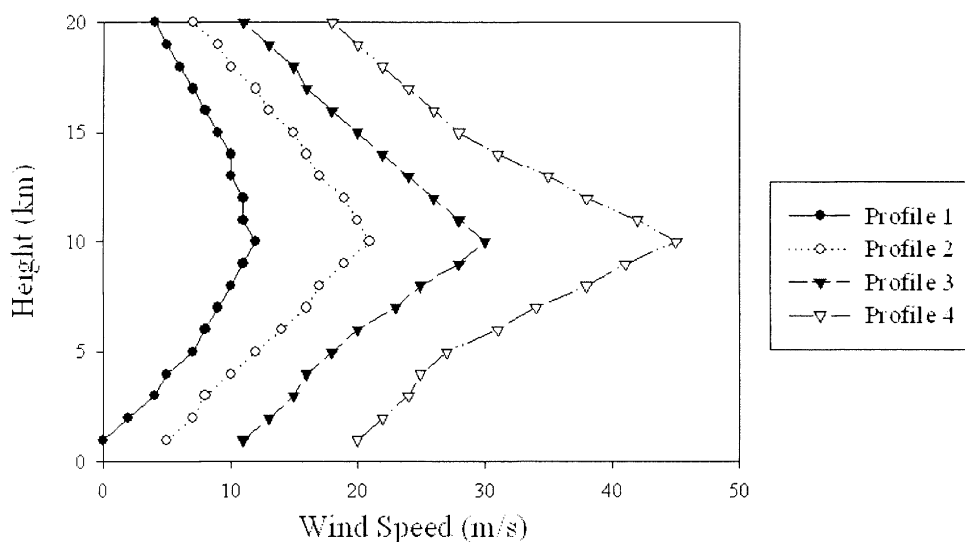


**Figure 2. Wind speed profiles.**

In all the profiles, wind speed is greatest near the tropopause (10 km) and decreases with distance above and below the tropopause. This is consistent with the commentary of Barry & Chorley (1992) who state that above the level of surface friction (500-1000 m), wind speed generally increases with height up to the tropopause, and decreases above it. Below

the level of surface friction, topographical features of the landscape will influence wind conditions causing them to be quite irregular, with poor correlation to wind conditions above 1000 m (Barry & Chorley, 1992). For this reason, wind speeds below 1000 m were not used in ASHFALL.

Although there is a general correlation between wind speed and height, there could be a significant variation between wind speeds at adjacent elevations so that at any given moment the wind variation might not fit into the general trend shown in Figure 2. The rate of change of wind speed with height is referred to as the wind shear. Above the level of surface friction, the wind shear will depend upon the temperature structure of the atmosphere, with small changes occurring with height (Barry & Chorley, 1992).

Nevertheless, the aim of the present exercise was to produce four wind speed profiles characterising the general nature of wind speeds over the North Island for use in ASHFALL, and which could be applied to different eruption sizes.

The probability of occurrence of each of the wind speed profiles is approximately equal to 0.25, or a 25% chance of occurrence, as a result of the derivation of the profiles from four approximately equal statistical quartiles, as described above.

Thus there are two probabilities associated with wind: the probability of a direction, and the probability of a velocity profile.

#### ASHFALL output

The output of ASHFALL is a two-dimensional grid file of ash thickness and is defined using the NZMS grid values as shown in Figure 1. A total of 12 grid files of ash thickness were produced, resulting from different eruption sizes and the four wind speed profiles. Screen and hardcopy plots of the grid files of ash thickness were made using Surfer<sup>®</sup> 7, a grid-based graphics program that interpolates irregularly spaced X/Y/Z coordinate data into a regularly spaced grid. The grid can then be used to produce contour maps of ash thickness.

Twelve contour maps of ash thickness were produced. Contour lines were drawn at ash thicknesses of 1, 2, 5, 10, 25 and 100 millimetres, where applicable. The geometry of each map varied between distributions retaining a degree of circular symmetry and those displaying a more ellipsoidal geometry where the wind speed was higher.

#### Variation of ash thickness with distance

The next step was to determine the spatial distribution of ash thickness. To do so, the ash thickness along the axis of maximum dispersal was obtained, after which the transverse (north-south) variation could be obtained at different points along the primary axis. The ash thickness vs. distance relationships along the primary axis for different eruption sizes and wind profiles is shown in Figure 3.

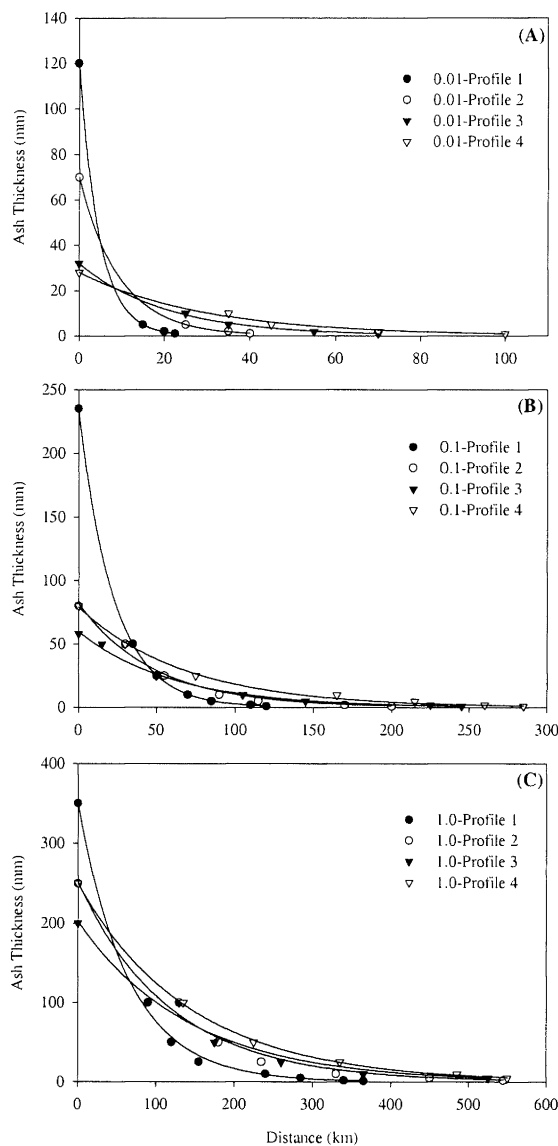


Figure 3. Ash thickness vs. distance relationships under four wind speed profiles for eruption sizes of (A) 0.01 km<sup>3</sup>, (B) 0.1 km<sup>3</sup> and (C) 1.0 km<sup>3</sup>.

The thickness vs. distance relationships showed an exponential relationship of the form

$$y = ae^{-bx}$$

with ash being dispersed to greater distances under high wind shear (Figure 3). At lower wind speeds there will be a greater ash thickness at the vent, with the largest eruption size modelled here (1.0 km<sup>3</sup>) resulting in a near-vent deposition in excess of 200 mm. However, when the fitted exponential curves for eruption sizes of 0.1 and 1.0 km<sup>3</sup> were

extrapolated to zero distance from the vent, the ash thicknesses for wind profiles 2 and 4 were very similar.

Cross sections of ash thickness were constructed at different longitudinal distances to determine the distribution of ash thickness transverse to the axis of maximum dispersal across a 45° sector. Figure 4 shows a typical result, in this case for an eruption of  $0.1 \text{ km}^3$  and a wind blowing from  $270^\circ$ . The cross sections were constructed approximately halfway between each contour of known ash thickness, with the thickness assumed to be half the thickness between the

downwind and upwind contours of known ash thickness, assuming an exponential decay of ash thickness as a function of distance. When constructing these cross sections it was also assumed that the ash thickness would decay to zero thickness, transverse to the axis of maximum dispersal, at 1 km from the Y coordinates defining the 1 mm contour. The geometries of the cross sections are roughly triangular, with the maximum ash thickness along the axis of maximum dispersal decreasing in a nearly linear fashion to zero thickness on either side (Figure 4).

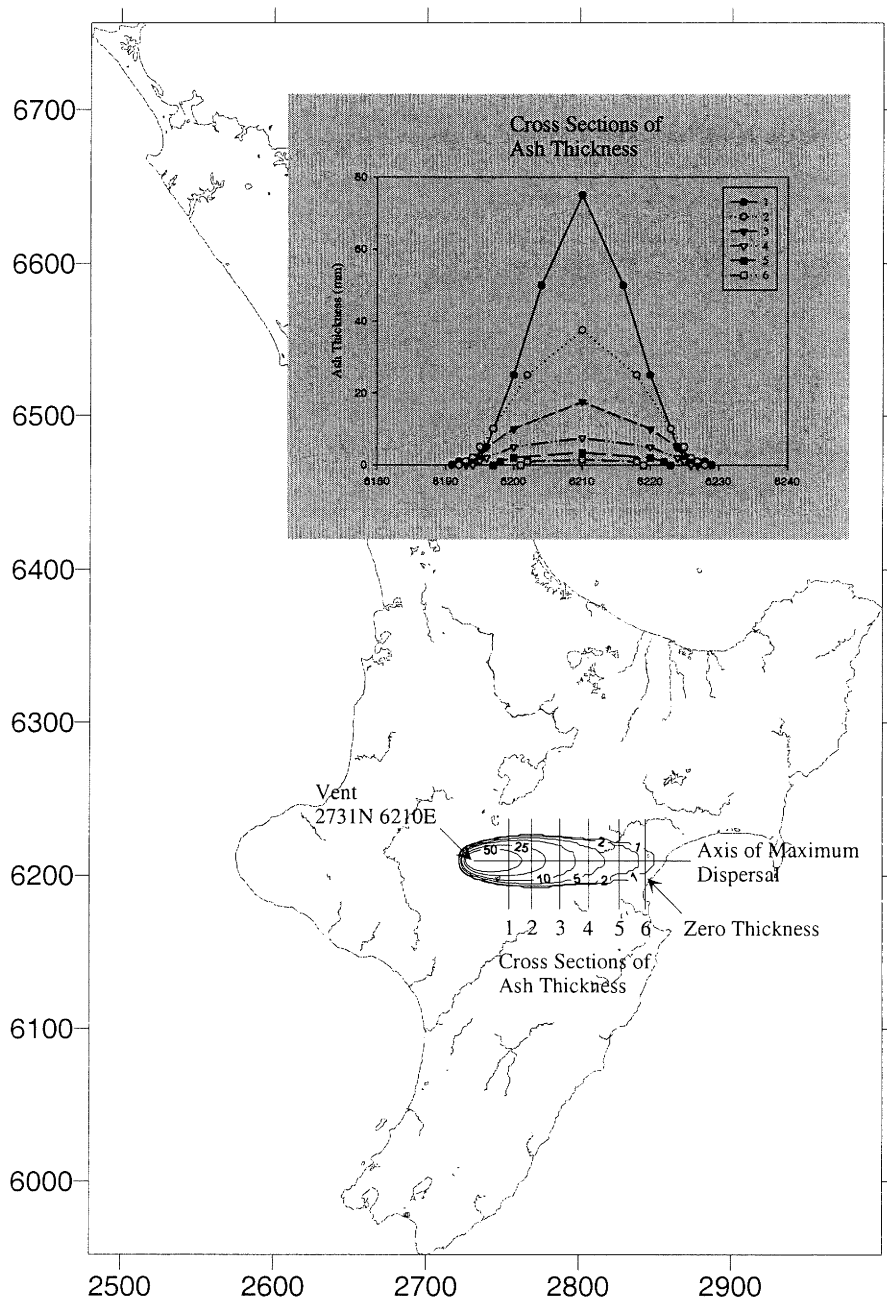


Figure 4. Cross sections of ash thickness for a  $0.1 \text{ km}^3$  eruption and Wind Speed Profile 1.

Next comes a significant simplifying step. To make it easier to calculate ash fall thickness probabilities, the total ash fall at any cross section is assumed to be distributed uniformly over a triangular sector radiating from the eruption site. This is shown in Figure 5, where two lines, in this case at  $45^\circ$  to each other, radiate from the vent. The ash is thus assumed to fall uniformly between the two lines. The angle between them is determined by looking at the pattern of deposition

shown by ASHFALL. Generally, higher winds lead to a longer and narrower zone of deposition. Figure 5 shows the limiting lines at  $45^\circ$  both because it will not be far from the truth in some cases, but also because the wind direction has been characterised by the probabilities of it occurring in eight  $45^\circ$  sectors. Where the ash plume is narrower, it is convenient to use a sector angle which is some definite fraction of  $45^\circ$ , such as  $15^\circ$ .

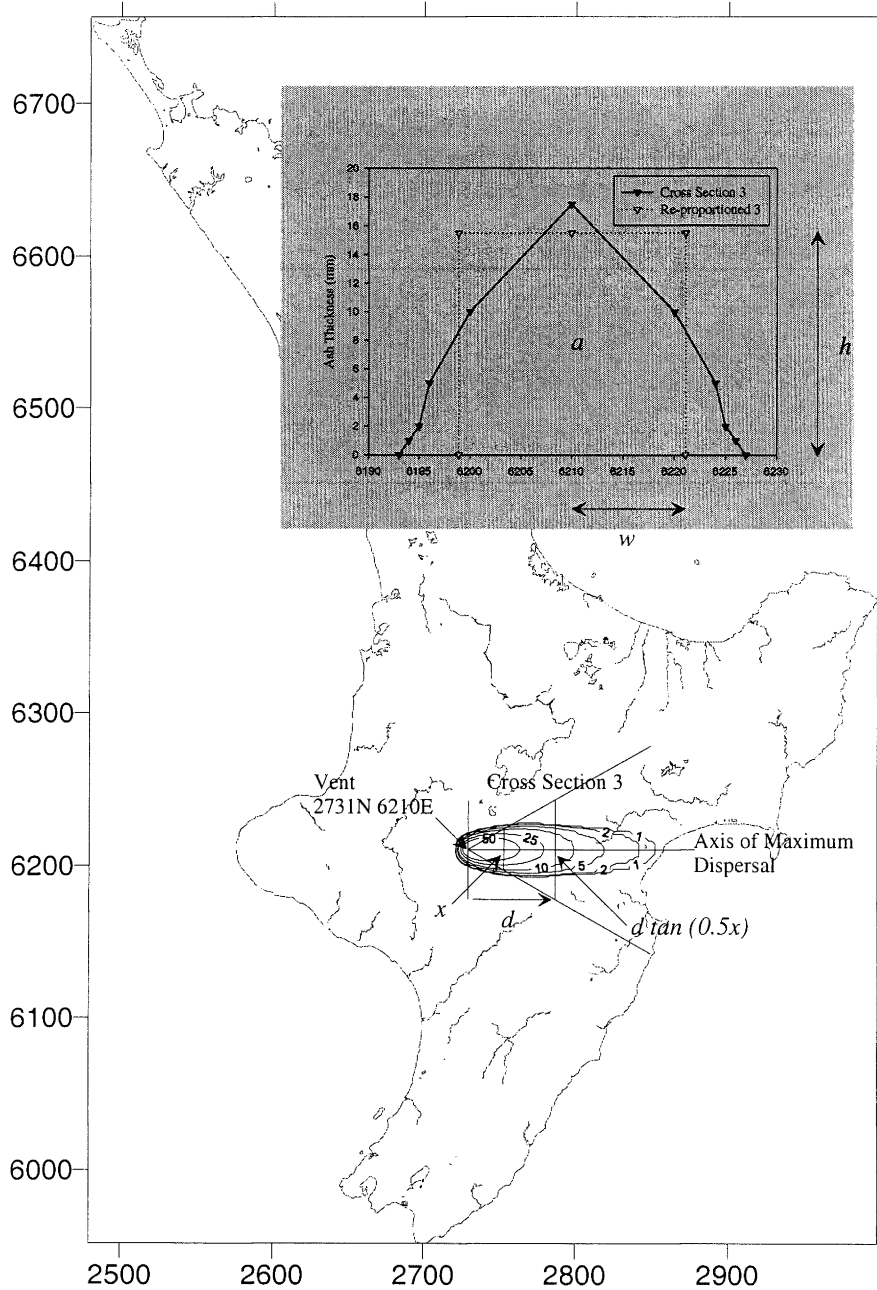


Figure 5. Schematic diagram of the procedure used to re-proportion the area of each of the cross sections to achieve an equivalent uniform distribution across in this case a  $45^\circ$  sector. Inset: the re-proportioned area of cross section 3 from an eruption size of  $0.1 \text{ km}^3$  modelled under wind speed profile 1, with the resultant width ( $w$ ) on either side of the axis of maximum dispersal, and height ( $h$ ).

Once the cross sections of ash thickness have been constructed, the area  $a$  of each cross section can be calculated. As shown in Figure 5, given the distance  $d$  of each cross section from the vent and the sector angle  $x$ , then the equivalent ash height  $h$  distributed uniformly either side of the axis of maximum dispersal and bounded by the sector angle is given by

$$h = \frac{a}{2d \tan(x/2)}$$

However, as stated above, different eruption sizes under each of the wind speed profiles will produce contour maps that will cover varying proportions of the area across a  $45^\circ$  sector. For example, under low wind shear, the lateral spreading of ash in the eruption column/cloud of a  $0.01 \text{ km}^3$  eruption will produce a contour map that retains a degree of circular symmetry and will cover most of the area across a  $45^\circ$  sector, whereas under high wind shear, the lateral spreading of ash in the eruption column/cloud of a  $0.01 \text{ km}^3$  eruption will produce a contour map that displays a more ellipsoidal geometry and will cover much less of the area across a  $45^\circ$  sector. In all but one case,  $45^\circ$  did not define the lateral spreading of ash in the eruption column/cloud and angles  $x$  of  $22.5$ ,  $15$  or  $11.25^\circ$  were chosen. Using such angles appeared to produce reasonable equivalent uniform thickness values across the relevant sectors.

Given a probability  $p$  of the wind being in a particular  $45^\circ$  sector, then the probability of the wind being in a sector of angle  $x$  within the  $45^\circ$  sector would be  $(x/45)p$ .

After the area of each of the cross sections was re-proportioned to achieve an equivalent uniform distribution across a  $45$ ,  $22.5$ ,  $15$  or  $11.25^\circ$  sector, ash thickness vs. distance relationships of the different eruption sizes under each of the wind speed profiles were re-drawn using the known distance from the vent of each of the cross sections. Again the ash thickness vs. distance relationships showed an exponential relationship of the form

$$y = ae^{-bd}$$

Ash is dispersed to greater distances under high wind speeds, decreasing in sequence to distances nearer the vent under low wind speed (Figure 6). However, when fitting exponential curves to eruption sizes of  $0.1$  and  $1.0 \text{ km}^3$ , the extrapolated maximum ash thickness at the vent now also decreased in sequence with increasing wind shear, which was not the case for the unmodified profiles of Figure 3.

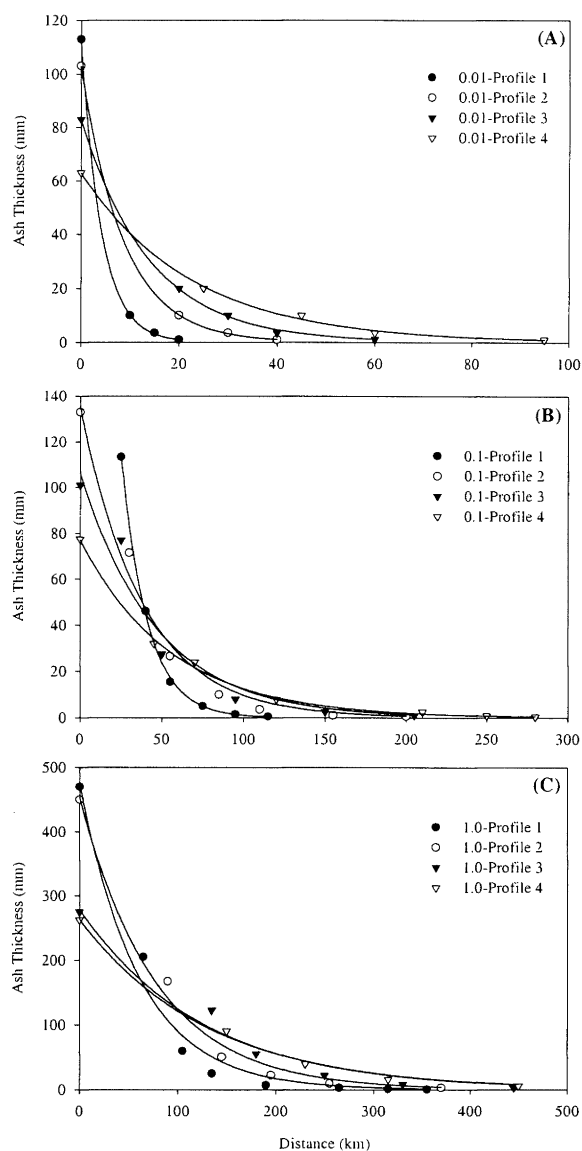


Figure 6. Re-proportioned ash thickness vs. distance relationships for eruption sizes: (A)  $0.01 \text{ km}^3$ , (B)  $0.1 \text{ km}^3$  and (C)  $1.0 \text{ km}^3$  for each wind speed profile.

## PROBABILITIES

Thus far the paper has been concerned with calculating the ash fall thickness distributions for known eruption sizes and wind characteristics. The analysis has been deterministic and there has been no consideration of uncertainty. Moreover,

the derivations have not taken into account different wind directions and have for convenience considered a westerly wind from one unspecified vent.

The next step is to introduce probabilistic considerations in order, ultimately, to obtain probability estimates of ash fall thickness in the Napier/Hastings area.

#### Annual probability vs. distance

In general, the effects of ash falls on human health, property and community lifelines primarily depend on the thickness of the ash that falls. Scott *et al.* (1998) summarised the effects of ash falls in terms of five levels of thickness to simplify any future analysis of ash fall hazards in the Hawke's Bay region. The ash thickness levels are: <1 mm, 1-5 mm, 5-50 mm, 50-100 mm and 100-300 mm. An ash thickness greater than 300 mm will have similar effects to one of 100-300 mm, but the effects will be amplified as ash thickness increases beyond 300 mm (Scott *et al.*, 1998). The five levels were adopted for use in this study.

Figure 6 shows curves representing 12 combinations of eruption size and wind profile. Let

- $p_{ei}$  = annual probability of eruption of a particular size for volcanic centre  $i$
- $p_{wi}$  = probability of wind profile during eruption of volcanic centre  $i$
- $p_{di}$  = probability of wind direction during eruption of volcanic centre  $i$
- $p_{ri}$  = proportion of 45° sector for to the above three events for centre  $i$

Then any one curve in Figure 6, for a particular wind direction, will have an annual probability of occurrence of

$$p_{ai} = p_{ei} p_{wi} p_{di} p_{ri}$$

Therefore, each of the twelve curves in Figure 6 represents the variation of thickness with distance with a probability  $p_{ai}$  for one wind direction and one volcanic centre.

#### Ash fall occurrence at Napier/Hastings

The next step is to find the probabilities of ash fall occurrence of various thicknesses in the Napier/Hastings region. The results can be obtained by adding the annual probabilities from the TgVC, EVC, TVC and OVC at the appropriate distances and wind directions. The Napier/Hastings area is roughly 120 km from the TgVC with an upwind direction 270-315°, 250 km from the EVC with an upwind direction 270-315°, and 120 km and 175 km respectively from the TVC and OVC with an upwind direction 315-360°.

Figure 6 gives the ash thicknesses at different distances for eruption magnitudes of 0.01, 0.1 and 1.0 km<sup>3</sup> respectively, regardless of the eruption source. To find the probability of an ash fall of a given thickness (say, 1 mm) in the Napier/Hastings area, we need a general relationship between ash fall thickness at that location and the probability of occurrence. Consider eruptions at the TgVC, for example, which is 120 km from Napier/Hastings. Figure 6 gives the ash fall thicknesses to be expected at 120 km for three eruption sizes and four wind profiles. However, as discussed above, the four wind profiles are assumed to occur with equal probability, so that we can take the average of the four values of ash thickness at 120 km for each eruption magnitude.

We now need a relationship between probability and ash fall thickness, assuming the point of interest is directly downwind of the eruption. Figure 6 essentially gives two points on such a relationship - for instance, only eruptions of 0.1 km<sup>3</sup> and 1.0 km<sup>3</sup> at the TgVC will deposit a significant fall of ash at a distance of 120 km. Frequencies of eruptions of different magnitudes at the different volcanic centres are given in Table 1. We now assume a linear relation between the logarithm of eruption probability and the logarithm of ash fall thickness for the particular distance being considered; for example 120 km for TgVC eruptions. This of course implies that there is a continuous distribution of possible eruption sizes. The assumed relation can be written

$$\log(p) = A + B \log(t)$$

where  $p$  and  $t$  are annual probability and thickness respectively, and  $A$  and  $B$  are constants. Because two points are known,  $A$  and  $B$  can be found.

This assumes the wind is blowing directly from the eruption to the Napier/Hastings area. This will not normally be the case, so we need to multiply the probability so far obtained by the probability of the wind being in the relevant sector. We can estimate this from the data given in Table 2. Here we have a difficulty. If we take a TgVC eruption as an example, the wind would have to be blowing from the 270-315° sector for ash to fall at the site of interest. Unfortunately, Table 2 assigns different probabilities to the sector for wind at different heights.

As the ash falls, it will of course be spending time at different heights. In the absence of a more detailed analysis we will use a single probability and assume that it is the average of those at 5 km and 10 km. Thus for a TgVC eruption we will use a wind direction probability of 0.3, which is roughly the average of the two figures of 0.27 and 0.34 given in Table 2.

We can now compute the annual probabilities of different ash fall thickness from the different sources and in total, as in Table 3, together with return periods. Note that because of the uncertainties introduced by data limitations and by the simplifying assumptions in the analysis, we must regard the

probabilities calculated as described above as median estimates. To give some idea of the effect of the uncertainties, the total median probabilities in Table 3 are multiplied by 0.5 and 1.5 to give low and high estimates, with a range of  $\pm 50\%$ . Thus the return period for a 1 mm fall of ash can be assumed to be somewhere in the range of 14 to 41 years.

Note that the contribution of the various volcanic centres to ash fall varies for the different thicknesses. There is very little probability that eruptions other than at the TgVC will

contribute to a 1 mm fall at Napier/Hastings. All other centres combined contribute less than 1% of the likelihood. Naturally, a very large eruption elsewhere could very well result in a substantial ash fall at Napier and Hastings, but the probability of such an eruption would be very small. However, the contribution of the other centres to larger ash falls is relatively greater. For a 5 mm fall, the other centres contribute about 6%, and for a 50 mm fall, about 60%.

**Table 3. Annual probabilities of ash fall of 1, 5 and 50 mm for the Napier/Hastings area, and the corresponding return periods, ( $E-5 = 10^{-5}$ ).**

Volcanic Centre	Ash fall thickness								
	1 mm			5 mm			50 mm		
	Low	Med.	High	Low	Med.	High	Low	Med.	High
TgVC	-	0.0487	-	-	0.00353	-	-	8.29E-5	-
EVC	-	0.00014	-	-	6.59E-5	-	-	2.21E-5	-
TVC	-	0.00014	-	-	7.63E-5	-	-	3.42E-5	-
OVC	-	7.84E-5	-	-	7.08E-5	-	-	6.12E-5	-
<b>Total</b>	<b>0.0245</b>	<b>0.0491</b>	<b>0.0736</b>	<b>0.0019</b>	<b>0.0037</b>	<b>0.0056</b>	<b>0.0001</b>	<b>0.0002</b>	<b>0.0003</b>
<b>R. Period (years)</b>	<b>41</b>	<b>20</b>	<b>14</b>	<b>534</b>	<b>267</b>	<b>178</b>	<b>9900</b>	<b>5000</b>	<b>3300</b>

## DISCUSSION

The results of the probabilistic ash fall model presented here have been derived from sometimes uncertain or limited data, so the limitations of the overall model need to be considered. This is particularly necessary with regard to possible development of the model in future as more data becomes available.

### Return Periods

The development of a model of annual ash fall probability is only possible if a return period can be defined for the different eruption sizes which could occur at the different volcanic centres. The North Island of New Zealand contains a number of rhyolitic and andesitic volcanic centres that have been active in the Quaternary, and much of their eruptive history has been defined from ash fall deposits preserved in lakes and bogs. Lakes and bogs preserve ash fall deposits, which could otherwise be difficult to trace or identify with certainty in sub-aerial environments, especially when affected by erosion (Lowe, 1988).

In the Hawkes Bay region, 37 ash fall deposits have been preserved in lakes and bogs; for example, Kaipo Bog near Lake Waikaremoana, Lake Tutira and Lake Poukawa (Howorth *et al.*, 1980; Eden *et al.*, 1993; Eden & Froggatt,

1996; Page & Trustrum, 1997; Lowe *et al.*, 1999). The ash fall deposits range from trace deposits (1 mm) to greater than 100 mm and can be grouped into the five levels of ash thickness discussed above. Scott *et al.* (1998) have defined magnitude/frequency relationships for the different volcanic centres from such ash fall deposits.

However, the lake and bog environments have apparently only preserved ash fall deposits that were widely distributed and with a large ash thickness. For example, there have been four explosive eruptions in the past 50 years from Mt. Ruapehu (1945, 1975, 1995 and 1996) that resulted in ash falls on Napier, but none was substantial enough to be detected in the Lake Tutira cores (Scott *et al.*, 1998). Consequently, large magnitude eruptions could be over represented due to the poor preservation of small magnitude eruption records.

It is also difficult to ascertain to what extent these ash fall deposits have been compacted. This would affect the five levels of ash thickness and hence the magnitude/frequency relationships defined by Scott *et al.* (1998). Studies have shown that the preserved ash thickness is usually less than 50% of the original ash thickness (Carey & Sigurdsson, 1982). There are therefore uncertainties in the magnitude/frequency relationships of the different volcanic centres used in the development of the model.

### Ash Thickness vs. Distance Relationships

The aggregation of fine ash particles may influence ash thickness vs. distance relationships, as aggregation can cause the premature settling of fine ash particles that would have otherwise been dispersed farther from the vent (Carey & Sigurdsson, 1982). The ash thickness vs. distance relationships of the 18 May 1980 eruption of Mt. St. Helens shows a well-defined zone of secondary ash thickening, which occurs between 250 and 350 km, near the city of Ritzville, Washington. This has been attributed to the aggregation of fine ash particles (Carey & Sigurdsson, 1982). It was not possible to consider the aggregation of fine ash particles and the influence on the ash thickness vs. distance relationships in the model.

### Eruption Sizes

The model also did not take into account eruption sizes greater than  $1.0 \text{ km}^3$ . Eruption sizes of 0.01, 0.1 and  $1.0 \text{ km}^3$  were taken into account and cover the range of likely eruption sizes from the TgVC and EVC, but do not cover the range of likely eruption size from the TVC and OVC. The range of likely eruption sizes from the TVC and OVC extend from  $1.0\text{-}100 \text{ km}^3$ , with uncertainties in the return periods for eruption sizes  $>1.0 \text{ km}^3$  (Table 1). Such an undertaking would require data on wind conditions above 20 km and greater certainty in the return periods for eruption sizes  $>1.0 \text{ km}^3$  from the TVC and OVC. Unfortunately, both NIWA and the Meteorological Service of New Zealand, Ltd. only collect wind direction and wind speed data up to 20 km, and only the structural and evolutionary history for the TVZ for the last 65,000 years, from which these return periods are defined, can be considered to be reasonably complete (Houghton *et al.*, 1995; Wilson *et al.*, 1995a).

However, a different way of looking at the situation is to say that the very large eruptions are exceedingly rare, and that the scale of damage experienced over a very large area of the country would be so great that any specific estimate of ash fall thickness at Napier/Hastings would be relatively meaningless. Omission of any consideration of very large eruptions in the present analysis is justified on these grounds.

### Wind

It was assumed that wind direction, speed and profile remained constant during the course of an eruption. This is unlikely to be so in practice. The effect of the assumption will be that ASHFALL will distribute more ash in a single direction, at times confined to a relatively narrow sector, whereas in reality it might be spread more widely during the full course of an eruption. It may be, from the probabilistic point of view, that the result will not be greatly affected. Nevertheless, the point needs to be examined further, and shows the need for more detailed information on the variation of wind conditions over time.

### Ash fall at the Napier/Hastings area

Table 3 shows a return period of between 14 and 40 years for a 1 mm fall of ash in the Napier/Hastings area. This is a relatively short return period. Typically local authorities in New Zealand design flood protection works for floods with return periods in the range 100-500 years, though overseas the design criteria are sometimes stricter. Holland, for instance, requires most of its river flood protection works against floods with a 1200 year return period. One interpretation of the result could therefore be that the ash fall hazard for the Napier/Hastings area is certainly of a magnitude which would justify expenditure on protective measures and civil defence and emergency management preparedness.

A 1 mm fall of ash is in fact very significant and would certainly be enough to cause health problems. It would also cause problems for the farming community and users of sensitive equipment. At that distance from eruption sites the ash would be very fine and pervasive. For this reason it might well be appropriate to consider a limit lower than 1 mm as a threshold requiring preparedness as well as intervention after the fact.

The physical consequences of relatively low levels of ash fall are not yet well understood. The issue could be significant, and more work needs to be done on the subject.

### Next steps

It would clearly be a relatively straightforward extension of the work reported here to develop contour maps for the North Island of expected ash fall depths for given return periods. Here, the analysis concentrated on finding ash fall return periods for a single location. The next step would be to repeat the analysis for a grid of points, from which the contours could be obtained by interpolation. Such maps would be useful for local authorities and industry, much as seismic hazard maps are used at present.

### CONCLUSION

The primary purpose of the research described in this paper was to establish the feasibility of a relatively simple model for estimating return periods of ash fall at different points in the North Island of New Zealand. The authors believe this aim has been achieved.

The research also produced estimates of ash fall return periods for the cities of Napier and Hastings, and it showed a need for further work in some areas, among other things to improve the quality of data.

A relatively straightforward extension of the work could result in contour maps of ash fall thickness at different return periods. Such a result would be useful for civil defence and emergency management planning purposes.

The work aimed to follow the principle of consistent crudeness and match the uncertainty in the model with that of the data. Hence, if more refined data were available the model itself could be further refined – the two must go hand in hand. Thus there is a need for further work both on the quality of the required data (such as time variation in wind direction, or the influence of turbulence) and also on the implications of some of the simplifying assumptions used in the analysis.

## REFERENCES

- Armienti, P., Macedonio, G. & Pareschi, M.T. (1988). "A numerical model for the distribution of tephra transport and deposition: applications to May 18, 1980 Mt. St. Helens eruption". *Journal of Geophysical Research*, **93**, 6463-6476.
- Barry, R.G. & Chorley, R.J. (1992). "Atmosphere, Weather and Climate". *Routledge, London*, 392p.
- Carey, S. & Sigurdsson, H. (1982). "Influence of particle aggregation on deposition of distal tephra from the May 18, 1980 eruption of Mount St. Helens volcano". *Journal of Geophysical Research*, **87**, 7061-7072.
- Carey, S. & Sigurdsson, H. (1989). The intensity of plinian eruptions. *Bulletin of Volcanology*, **51**, 28-40.
- Carey, S. & Sparks, R.S.J. (1986). "Quantitative models of the fallout and dispersal of tephra from volcanic eruption columns". *Bulletin of Volcanology*, **48**, 109-125.
- Cornell, C.A. (1968). "Engineering seismic risk analysis". *Bulletin of the Seismological Society of America*, **58**, 1583-1606.
- Dalziel, E. (1998). "Risk assessment methods in road network evaluation: a study of the impact of natural hazards on the Desert Road, New Zealand". PhD Thesis, *University of Canterbury*, Christchurch, New Zealand.
- Eden, D.N., Froggatt, P.C., Trustrum, N.A. & Page, M.J. (1993). "A multiple-sourced Holocene tephra sequence from Lake Tutira, Hawke's Bay, New Zealand". *New Zealand Journal of Geology and Geophysics*, **36**, 233-242.
- Eden, D.N. & Froggatt, P.C. (1996). "A 6,500 year old history of tephra deposition recorded in the sediments of Lake Tutira, Eastern North Island, New Zealand". *Quaternary International*, 34-36, 55-64.
- Elms, D.G. (1992). "Consistent crudeness in system construction". In B.H.V. Topping (Ed), *Optimisation and Artificial Intelligence in Civil Engineering*, Kluwer Academic Publishers, v.1, 61-70.
- Houghton, B.F., Wilson, C.J.N., McWilliams, M.O., Lanphere, M.A., Weaver, S.D., Briggs, R.M. & Pringle, M.S. (1995). "Chronology and dynamics of a large silicic magmatic system: Central Taupo Volcanic Zone, New Zealand". *Geology*, **23**, 13-16.
- Howorth, R., Froggatt, P.C. & Robertson, S.M. (1980). "Late Quaternary volcanic ash stratigraphy of the Poukawa area, Central Hawke's Bay, New Zealand". *New Zealand Journal of Geology and Geophysics*, **23**, 487-491.
- Hurst, A.W. (1994). "ASHFALL – A computer program for estimating volcanic ash fallout: report and users guide". *Science Report 94/23. Institute of Geological and Nuclear Sciences*.
- Hurst, A.W. & Turner, R. (1999). "Performance of the program ASHFALL for forecasting ashfall during the 1995 and 1996 eruptions of Ruapehu volcano". *New Zealand Journal of Geology & Geophysics*, **42**, 615-622.
- Johnston, D.M. & Nairn, I.A. (1993). "Volcanic impacts report: the impact of two eruption scenarios from the Okataina Volcanic Centre on the population and infrastructure of the Bay of Plenty Region, New Zealand". *Resource Planning Publication 93/6. Bay of Plenty Regional Council*.
- Johnston, D.M. (1997). "Physical and social impacts of past and future volcanic eruptions in New Zealand". Ph.D. Thesis, *Massey University*, Palmerston North, New Zealand.
- Latter, J.H. (1985). "Frequency of eruptions at New Zealand volcanoes". *Bulletin of the New Zealand National Society for Earthquake Engineering*, **18**, 55-110.
- Lowe, D.J. (1988). "Late Quaternary volcanism in New Zealand: towards an integrated record using distal airfall tephra in lakes and bogs". *Journal of Quaternary Science*, **3**(2), 111-120.
- Lowe, D.J., Newham, R.M. & Ward, C.M. (1999). "Stratigraphy and chronology of a 15 ka sequence of multi-sourced silicic tephra in a montane peat

- bog, Eastern North Island, New Zealand". *New Zealand Journal of Geology and Geophysics*, **42**, 565-579.
- Macedonio, G., Pareschi, M.T. & Sanatacroce, R. (1988). "A numerical simulation of the plinian fall phase of 79A.D. eruption of Vesuvius". *Journal of Geophysical Research*, **93**, 14817-14827.
- Newhall, C.G. & Self, S. (1982). "The Volcanic Explosivity Index (VEI): An estimate of explosive magnitude for historical volcanism". *Journal of Geophysical Research*, **87**, 1231-1238.
- Page, M.J. & Trustrum, N.A. (1997). "A late Holocene lake sediment record of the erosion response to land use changes in a steep land catchment, New Zealand". *Geomorphology*, **41**:3, 369-392.
- Rhoades, D.A., Dowrick, D.J. & Wilson, C.J.N. (2002). "Volcanic hazard in New Zealand: Scaling and attenuation relations for tephra fall deposits from Taupo Volcano". *Natural Hazards*, **26**, 147-174.
- Scott, B.J., Johnston, D.M. & Manville, V. (1998). "Volcanic impacts in the Hawke's Bay region". *Client Report 71754D.10. Institute of Geological and Nuclear Sciences*.
- Stirling, M., Yetton, M., Petinga, J., Berryman, K. & Downes, G. (1999). "Probabilistic seismic hazard assessment and earthquake scenarios for the Canterbury Region, and Historic Earthquakes in Christchurch". *Client Report 1999/53. Institute of Geological and Nuclear Sciences*.
- Sturman, A.P. & Tapper, N.J. (1996). "The Weather and Climate of Australia and New Zealand". *Oxford University Press*, Melbourne, 476p.
- Wilson, C.J.N., Houghton, B.F., McWilliams, M.O., Lanphere, M.A., Weaver, S.D. & Briggs, R.M. (1995). "Volcanic and structural evolution of Taupo Volcanic Zone, New Zealand: a review". *Journal of Volcanology and Geothermal Research*, **68**, 1-28.